Kinematic and dynamic modeling of spherical joints using exponential coordinates

Jinwook Kim, Sung-Hee Lee and Frank C Park

Proceedings of the Institution of Mechanical Engineers, Part C: Journal of Mechanical Engineering Science 2014 228: 1777 originally published online 24 November 2013
DOI: 10.1177/0954406213511365

Original Article

Institution of MECHANICAL ENGINEERS
Journal of MECHANICAL ENGINEERING SCIENCE

Proc IMechE Part C:
J Mechanical Engineering Science
2014, Vol. 228(10) 1777–1785

DOI: 10.1177/0954406213511365
pic.sagepub.com
SAGE

Kinematic and dynamic modeling of spherical joints using exponential coordinates

Jinwook Kim[1], Sung-Hee Lee[2] and Frank C Park[3]

Abstract

Traditional Euler angle-based methods for the kinematic and dynamic modeling of spherical joints involve highly complicated formulas that are numerically sensitive, with complex bookkeeping near local coordinate singularities. In this regard, exponential coordinates are known to possess several advantages over Euler angle representations. This paper presents several new exponential coordinate-based formulas and computational procedures that are particularly useful in the modeling of mechanisms containing spherical joints. Computationally robust procedures are derived for evaluating the forward and inverse formulas for the angular velocity and angular acceleration in terms of exponential coordinates. We show that these formulas simplify the parametrization of joint range limits for spherical joints, and lead to more compact equations in the forward and inverse dynamic analysis of mechanisms containing spherical joints.

Keywords

Exponential coordinates, spherical joint, rotation, parallel mechanism

Date received: 15 February 2013; accepted: 10 October 2013

Introduction

The need to model and simulate spherical (also ball-and-socket) joints arises in a wide range of applications, ranging from the simulation and control of parallel robotic structures like the Stewart–Gough platform, to the simulation of biomechanical joints like the human shoulder joint. Typically the spherical joint is kinematically modeled as a series of three revolute (3 R) joints, arranged such that the three joint axes intersect orthogonally at a common point (in some biomechanical models the axes are not always orthogonal to each other).

The drawbacks with such a model are of course well known: whenever the first and third joint axes are collinear, the 3 R model is at a kinematic singularity (i.e., the model is unable to instantaneously rotate about certain directions), when in fact the actual spherical joint experiences no such singularity. Also, expressing the spherical joint's range of motion, which is most naturally done in terms of a reach cone, becomes highly complicated and unwieldy using the 3 R model. This can significantly impact the accuracy and efficiency of dynamic simulations, particularly for high-speed motions, in which the repulsive impulse—generated when a spherical joint reaches a joint limit—needs to be accounted for in the dynamic simulation.[1,2]

In this paper, we investigate the suitability of the exponential coordinates, also widely known as the Rodrigues parameters, as a model for spherical joints. The exponential coordinates are a well-known and extensively used set of local coordinates for parametrizing the rotations that overcome many of the disadvantages associated with Euler angle representations. Using the exponential coordinates, a rotation can be visualized intuitively by its unit axis of rotation $\hat{\mathbf{r}} \in \Re^3$, $\|\hat{\mathbf{r}}\| = 1$, together with a rotation (in the right-hand sense) by an angle $\theta \in [0, 2\pi]$ about the axis. By defining $\mathbf{r} = \hat{\mathbf{r}}\theta \in \Re^3$, a three-parameter

[1]Imaging Media Research Center, Korea Institute of Science and Technology, Korea
[2]Graduate School of Culture Technology, Korea Institute of Science and Technology, Korea
[3]School of Mechanical and Aerospace Engineering, Seoul National University, Korea

Corresponding author:
Sung-Hee Lee, Graduate School of Culture Technology, Korea Institute of Science and Technology, Yuseong-gu, Daejeon 305-701, Republic of Korea.
Email: sunghee.lee@kaist.ac.kr

local coordinate parametrization for rotations is obtained. Forward and inverse formulas for the angular velocity in terms of $\mathbf{r}$ are known, as are their relation to, e.g., Cayley-Rodrigues parameters and unit quaternion representations.[3–6]

What has not been investigated, however, at least in a systematic way, are the numerical robustness and accuracy issues involved with using exponential coordinates in the modeling and simulation of spherical joints. In particular, the effective representation of spherical joint range limits and the determination of repulsive impulse generated when a spherical joint reaches its joint limit are clearly important issues in the dynamic simulation of mechanisms containing spherical joints. Numerically robust and efficient forward and inverse formulas for the angular acceleration are also important for dynamic simulation purposes.

The specific contributions of this paper are as follows:

- The forward and inverse formulas for the angular velocity $\mathbf{w}$ as a function of the exponential coordinates $\mathbf{r}$ and its time derivative $\dot{\mathbf{r}}$, i.e., $\mathbf{w} = \mathbf{J}(\mathbf{r})\dot{\mathbf{r}}$ and $\dot{\mathbf{r}} = \mathbf{G}(\mathbf{r})\mathbf{w}$ appear in the literature, but closed-form versions of these formulas are typically rational, potentially leading to divide-by-zero induced numerical instabilities when $\mathbf{r}$ is small. Here we provide numerically robust procedures for computing $\mathbf{w}$ and $\dot{\mathbf{r}}$ in such cases.
- We also derive a similar set of numerically robust computational procedures for the forward and inverse angular acceleration, i.e., $\dot{\mathbf{w}} = \mathbf{J}\ddot{\mathbf{r}} + \dot{\mathbf{J}}\dot{\mathbf{r}}$ and $\ddot{\mathbf{r}} = \mathbf{G}\dot{\mathbf{w}} + \dot{\mathbf{G}}\mathbf{w}$.
- By representing spherical joint range limits in terms of the exponential coordinates, we derive a compact formula for the repulsive impulse (more specifically, its direction) generated when a spherical joint reaches its joint limit.
- All three-parameter coordinate representations for rotations have coordinate singularities (the exponential coordinates are no exception; singularities occur when $\|\mathbf{r}\| = 2\pi, 4\pi$, etc.). It is well-known that at such singularities one must switch to different coordinate parametrizations.[7] For dynamic simulation of the spherical joints, $\dot{\mathbf{r}}$, $\ddot{\mathbf{r}}$, and joint torque need to be reparametrized as well. Here we derive simple and straightforward procedures for such coordinate reparametrizations.

The remainder of this paper is organized as follows. After reviewing related work in the next section and the preliminary formulas for exponential coordinates in section "Background," we derive the first and second-order differential relations between the rotation group and the exponential coordinates in section "Differential relation formulas for modeling spherical joints." Section "Spherical joint modeling and simulation" presents a joint range limit analysis and reparametrization schemes for the velocity, acceleration, and torques. The last section concludes the paper.

Related work

There is extensive literature on local coordinate parametrizations for rotation matrices (or more formally, the rotation group $SO(3)$), including formulas for the angular velocity in terms of the local coordinates.[3–5,8–16] Angular acceleration formulas in terms of the local coordinates have received less attention; this is also true in the case of exponential coordinates.[6,17,18] For almost all of the local coordinates (including exponential coordinates), existing analytic formulas for the angular velocity (and accelerations in a few limited cases) typically involve rational expressions that have a $\|\mathbf{r}\|$ term in the denominator (here $\mathbf{r} \in \Re^3$ denotes the local coordinates), which are numerically unstable when $\mathbf{r}$ approaches zero. In this paper, we derive numerically robust Taylor expansion-based procedures that address this case, for both the exponential coordinate-based angular velocity and angular acceleration.

Grassia[7] shows that the range of motion of spherical joints can be compactly expressed in terms of the exponential coordinates. Biological joints, unlike their mechanical counterparts, often have a complex range of motion. Engin and Tumer[19,20] develop a joint sinus cone model which allows the human shoulder joint to be more accurately modeled as a spherical joint. Wilhelms and Gelder[21] develop joint reach cone models that define the range of motion spherical joints in terms of a polygon that approximates a closed curve defined on the unit sphere. Lee and Terzopoulos[22] introduce a general scleronomic joint model by incorporating spline curves and surfaces to the modeling of joints. These works do not explicitly address dynamic modeling of the spherical joints under a limited range of motion. In this paper, we show that with the exponential coordinates, not only can joint range limits be conveniently expressed, but repulsive impulses generated at the joint limits during dynamic simulation can also be easily calculated.

Near coordinate singularities the usual practice is to switch to a different coordinate parametrization, and Grassia[7] derives a scheme for reparametrization of exponential coordinates. For dynamic simulation purposes, however, not only the coordinates but also their first- and second-order derivatives must also be reparametrized as well. In this paper, we derive reparametrizations for the exponential coordinates and their derivatives, as well as joint torques in the event that the spherical joint is actuated.

Background

We first review the basic properties of the exponential coordinates on $SO(3)$; these are well-documented in

Refs. 4, 18. Given $\mathbf{r} = (r_1, r_2, r_3) \in \Re^3$, denote its 3×3 skew-symmetric representation by $[\mathbf{r}]$, i.e.,

$$[\mathbf{r}] = \begin{bmatrix} 0 & -r_3 & r_2 \\ r_3 & 0 & -r_1 \\ -r_2 & r_1 & 0 \end{bmatrix} \tag{1}$$

The matrix exponential of $[\mathbf{r}]$ results in a proper rotation matrix, i.e., an element of $SO(3)$, whose explicit form is given analytically by Rodrigues formula:

$$\exp([\mathbf{r}]) = \mathbf{I} + \alpha[\mathbf{r}] + \beta[\mathbf{r}]^2 = \cos\theta \cdot \mathbf{I} + \alpha[\mathbf{r}] + \beta\mathbf{r}\mathbf{r}^T \tag{2}$$

where $\theta = \|\mathbf{r}\|$ and $\alpha = \sin\theta/\theta$, $\beta = (1 - \cos\theta)/\theta^2$.

Given a rotation matrix $\mathbf{R} \in SO(3)$, there exist exponential coordinates $\mathbf{r} \in \Re^3$ such that $\exp([\mathbf{r}]) = \mathbf{R}$ and its magnitude θ is bound to $[0, \pi]$. We can compute $\mathbf{r}$ by examining the matrix elements of equation (2),

$$\exp([\mathbf{r}]) = \begin{bmatrix} \beta r_1^2 + \cos\theta & \beta r_1 r_2 - \alpha r_3 & \beta r_1 r_3 + \alpha r_2 \\ \beta r_1 r_2 + \alpha r_3 & \beta r_2^2 + \cos\theta & \beta r_2 r_3 - \alpha r_1 \\ \beta r_1 r_3 - \alpha r_2 & \beta r_2 r_3 + \alpha r_1 & \beta r_3^2 + \cos\theta \end{bmatrix}$$

θ can be easily computed from the trace of $\mathbf{R}$:

$$\theta = \cos^{-1}\left(\frac{\mathrm{tr}\mathbf{R} - 1}{2}\right) \tag{3}$$

If $\theta \neq \pi$, we get

$$\mathbf{r} = \frac{1}{2\alpha}\begin{bmatrix} R_{32} - R_{23} \\ R_{13} - R_{31} \\ R_{21} - R_{12} \end{bmatrix} \tag{4}$$

where R_{ij} denotes the (i,j)-element of $\mathbf{R}$. Note that $\frac{1}{2\alpha}$ is well-defined at $\theta = 0$ and it can be approximated as $\frac{1}{2\alpha} \simeq \frac{1}{2} + \frac{\theta^2}{12}$ using the Taylor series expansion.

If θ is close to π, $1/\alpha$ is ill-defined and thus $\mathbf{r}$ should be calculated differently. From the diagonal entries of $\mathbf{R}$, we have

$$\mathbf{r} = \begin{bmatrix} \mathrm{sgn}(r_1)\sqrt{\frac{R_{11} - \cos\theta}{\beta}} \\ \mathrm{sgn}(r_2)\sqrt{\frac{R_{22} - \cos\theta}{\beta}} \\ \mathrm{sgn}(r_3)\sqrt{\frac{R_{33} - \cos\theta}{\beta}} \end{bmatrix} \text{ for } \theta \approx \pi \tag{5}$$

when $\theta \neq \pi$, the sign of r_1 can be determined by examining $R_{32} - R_{23} = 2\alpha r_1$. Since $\alpha > 0$ when $\theta \in [0, \pi)$, we have $\mathrm{sgn}(r_1) = \mathrm{sgn}(R_{32} - R_{23})$. Likewise, $\mathrm{sgn}(r_2) = \mathrm{sgn}(R_{13} - R_{31})$ and $\mathrm{sgn}(r_3) = \mathrm{sgn}(R_{21} - R_{12})$. When $\theta = \pi$, $\exp([\mathbf{r}]) = \exp([-\mathbf{r}])$, and $\mathbf{R}$ is symmetric. Therefore $R_{ij} - R_{ji} = 0$ and the signs of r_k $(i, j, k \in \{1, 2, 3\})$ cannot be determined using the above method. In this case, we can pick a diagonal entry $R_{ii} (\neq -1)$ and assign any sign to r_i. Then the signs of r_j and r_k can be determined from $R_{ij} = (2/\pi^2) r_i r_j$ and $R_{ik} = (2/\pi^2) r_i r_k$. The sign of r_i can be determined to keep the continuity of coordinates if desired.

Differential relation formulas

The angular velocity in the moving frame (*body angular velocity*), $\mathbf{w}_b \in \Re^3$, defined as $[\mathbf{w}_b] = \mathbf{R}^T\dot{\mathbf{R}}$, is expressed in terms of exponential coordinates:

$$\mathbf{w}_b = \alpha\dot{\mathbf{r}} + \beta\dot{\mathbf{r}} \times \mathbf{r} + \gamma\langle\mathbf{r}, \dot{\mathbf{r}}\rangle\mathbf{r} \tag{6}$$

where $\langle\cdot,\cdot\rangle$ denotes the standard Euclidean inner product in $\Re^3$, and

$$\gamma = \frac{\theta - \sin\theta}{\theta^3} = \frac{1 - \alpha}{\theta^2} \tag{7}$$

Equation (6) can be derived by substituting equation (2) for $\mathbf{R}^T$ and $\dot{\mathbf{R}}$ in $[\mathbf{w}_b] = \mathbf{R}^T\dot{\mathbf{R}}$ and simplifying terms by making use of the following general identities for arbitrary $\mathbf{r}, \mathbf{s} \in \Re^3$:

$$[\mathbf{r}]\mathbf{r} = \mathbf{0} \tag{8}$$

$$[\mathbf{r}]^2 = \mathbf{r}\mathbf{r}^T - \|\mathbf{r}\|^2\mathbf{I} \tag{9}$$

$$[\mathbf{r}]^3 = -\|\mathbf{r}\|^2[\mathbf{r}] \tag{10}$$

$$[\mathbf{r}][\mathbf{s}] = \mathbf{s}\mathbf{r}^T - \langle\mathbf{r}, \mathbf{s}\rangle\mathbf{I} \tag{11}$$

$$[\mathbf{r} \times \mathbf{s}] = [\mathbf{r}][\mathbf{s}] - [\mathbf{s}][\mathbf{r}] \tag{12}$$

$$\langle\dot{\mathbf{r}}, \mathbf{r}\rangle = \dot{\theta}\theta \tag{13}$$

Using the following relations

$$\mathbf{R}\mathbf{r} = (\mathbf{I} + \alpha[\mathbf{r}] + \beta[\mathbf{r}]^2)\mathbf{r} = \mathbf{r}$$

$$\mathbf{R}\dot{\mathbf{r}} = \cos\theta\dot{\mathbf{r}} + \alpha\mathbf{r} \times \dot{\mathbf{r}} + \beta\langle\mathbf{r}, \dot{\mathbf{r}}\rangle\mathbf{r}$$

$$\mathbf{R}(\mathbf{r} \times \dot{\mathbf{r}}) = \cos\theta\mathbf{r} \times \dot{\mathbf{r}} + \alpha\langle\mathbf{r}, \dot{\mathbf{r}}\rangle\mathbf{r} - \alpha\theta^2\dot{\mathbf{r}}$$

we can also relate $\dot{\mathbf{r}}$ with the angular velocity with respect to the fixed frame (*spatial angular velocity*), defined as $[\mathbf{w}_s] = \dot{\mathbf{R}}\mathbf{R}^T$, or $\mathbf{w}_s = \mathbf{R}\mathbf{w}_b$

$$\mathbf{w}_s = \alpha\dot{\mathbf{r}} - \beta\dot{\mathbf{r}} \times \mathbf{r} + \gamma\langle\mathbf{r}, \dot{\mathbf{r}}\rangle\mathbf{r} \tag{14}$$

Note that the equations (6) and (14) for $\mathbf{w}_b$ and $\mathbf{w}_s$ differ only in the sign of the second term.

If the inboard link of a spherical joint is moving, $\mathbf{w}_b$ and $\mathbf{w}_s$ represent the relative velocities of a child link with respect to its parent link, and $\mathbf{w}_b$ is frequently used for kinematic and dynamic analysis.[23] If a spherical joint is attached to a fixed link, $\mathbf{w}_s$ provides more intuitive expression for the velocity than $\mathbf{w}_b$ as $\mathbf{w}_s$ is expressed in the spatial frame.

Differential relation formulas for modeling spherical joints

We have presented formulas for the exponential coordinates and the first-order differential relations that have been introduced in the literature. We now present additional differential formulas that are essential for kinematic analysis and dynamic simulation of the spherical joints. Obviously, these formulas are useful for other problems related with the differential geometric operations for the rotation group (e.g., optimal trajectory generation problem[24]). First, we derive the inverse differential relations from the angular velocity to the derivative of the exponential coordinates: the relations can be used for solving the inverse kinematics of spherical joints. Second, we present the Jacobian matrices between the derivatives of exponential coordinates and the angular velocities. The Jacobian matrices are not only useful for the kinematic operations but also essential for solving gradient-based optimization problems for the mechanisms containing spherical joints. After that, we derive the second-order differential relations for the dynamic simulation of the spherical joints. Note that all these formulas contain $\|\mathbf{r}\|$ in the denominator, which many cause the divide-by-zero error when $\mathbf{r}$ becomes close to zero. Therefore, we derive the Taylor expansion-based formulas that allow for the robust computation of the differential formulas near $\mathbf{r} = \mathbf{0}$.

Inverse differential relations

Let us now express $\dot{\mathbf{r}}$ in terms of $\mathbf{w}_b$ or $\mathbf{w}_s$. From equation (6), we can derive the following equations:

$$\dot{\mathbf{r}} = \delta \mathbf{w}_b + \frac{1}{2}\mathbf{r} \times \mathbf{w}_b + \zeta \langle \mathbf{r}, \mathbf{w}_b \rangle \mathbf{r} \tag{15}$$

$$\dot{\mathbf{r}} = \delta \mathbf{w}_s - \frac{1}{2}\mathbf{r} \times \mathbf{w}_s + \zeta \langle \mathbf{r}, \mathbf{w}_s \rangle \mathbf{r} \tag{16}$$

where

$$\delta = \frac{\alpha}{2\beta}, \quad \zeta = \frac{1-\delta}{\theta^2} \tag{17}$$

Equation (15) can be derived as follows. Rearranging equation (6), we get

$$\dot{\mathbf{r}} = (\alpha \mathbf{I} - \beta[\mathbf{r}])^{-1}\left(\mathbf{w}_b - \gamma \langle \mathbf{r}, \dot{\mathbf{r}} \rangle \mathbf{r}\right)$$

To simplify the above equation, we apply the following relations that can be verified straightforwardly.

$$\begin{aligned} \langle \mathbf{r}, \mathbf{w}_b \rangle &= (\alpha + \gamma\theta^2)\langle \mathbf{r}, \dot{\mathbf{r}} \rangle = \langle \mathbf{r}, \dot{\mathbf{r}} \rangle \\ (\mathbf{I} + [\mathbf{r}])^{-1} &= \frac{1}{1 + \|\mathbf{r}\|^2}\left(\mathbf{I} - [\mathbf{r}] + \mathbf{r}\mathbf{r}^T\right) \end{aligned} \tag{18}$$

Then the mapping from $\mathbf{w}_b$ to $\dot{\mathbf{r}}$ can be expressed as follows:

$$\begin{aligned} \dot{\mathbf{r}} &= (\alpha \mathbf{I} - \beta[\mathbf{r}])^{-1}(\mathbf{w}_b - \gamma \langle \mathbf{r}, \dot{\mathbf{r}} \rangle \mathbf{r}) \\ &= \frac{\sin^2\theta}{2\alpha(1-\cos\theta)}\left(\mathbf{I} + \frac{\beta}{\alpha}[\mathbf{r}] + \frac{\beta^2}{\alpha^2}\mathbf{r}\mathbf{r}^T\right)(\mathbf{w}_b - \gamma \langle \mathbf{r}, \mathbf{w}_b \rangle \mathbf{r}) \\ &= \delta \mathbf{w}_b + \frac{1}{2}\mathbf{r} \times \mathbf{w}_b + \zeta \langle \mathbf{r}, \mathbf{w}_b \rangle \mathbf{r} \end{aligned} \tag{19}$$

where

$$\delta = \frac{\sin^2\theta}{2\alpha(1-\cos\theta)} = \frac{\alpha}{2\beta}$$

and

$$\zeta = \delta\left(\frac{\beta^2}{\alpha^2} - \gamma - \gamma\theta^2\frac{\beta^2}{\alpha^2}\right) = \frac{1-\delta}{\theta^2}$$

Jacobian matrices

By manipulating equation (6), we can derive a Jacobian matrix $\mathbf{J}_b(\mathbf{r}) \in \Re^{3\times 3}$ that maps the first derivative of the exponential coordinates to that of a rotation matrix, i.e., $\mathbf{J}_b = \mathbf{R}^T \frac{\partial \mathbf{R}}{\partial \mathbf{r}}$, or equivalently $\mathbf{w}_b = \mathbf{J}_b(\mathbf{r})\dot{\mathbf{r}}$

$$\mathbf{J}_b(\mathbf{r}) = \alpha \mathbf{I} - \beta[\mathbf{r}] + \gamma \mathbf{r}\mathbf{r}^T \tag{20}$$

$$= \mathbf{I} - \beta[\mathbf{r}] + \gamma[\mathbf{r}]^2 \tag{21}$$

Equation (21) is derived from equation (20) by using the relation equation (9). In the event that $\mathbf{J}_b(\mathbf{r})$ is invertible, denote $\mathbf{J}_b^{-1}(\mathbf{r}) = \mathbf{G}_b(\mathbf{r})$, so that $\dot{\mathbf{r}} = \mathbf{G}_b(\mathbf{r})\mathbf{w}_b$. $\mathbf{G}_b(\mathbf{r})$ can be acquired by rearranging terms in equation (15):

$$\begin{aligned} \mathbf{G}_b(\mathbf{r}) &= \delta \mathbf{I} + \frac{1}{2}[\mathbf{r}] + \zeta \mathbf{r}\mathbf{r}^T \\ &= \mathbf{I} + \frac{1}{2}[\mathbf{r}] + \zeta[\mathbf{r}]^2 \end{aligned} \tag{22}$$

One can also write $\mathbf{w}_s = \mathbf{J}_s(\mathbf{r})\dot{\mathbf{r}}$ and $\dot{\mathbf{r}} = \mathbf{G}_s(\mathbf{r})\mathbf{w}_s$, where

$$\mathbf{J}_s(\mathbf{r}) = \alpha \mathbf{I} + \beta[\mathbf{r}] + \gamma \mathbf{r}\mathbf{r}^T \tag{23}$$

$$= \mathbf{I} + \beta[\mathbf{r}] + \gamma[\mathbf{r}]^2 \tag{24}$$

$$\begin{aligned} \mathbf{G}_s(\mathbf{r}) &= \delta \mathbf{I} - \frac{1}{2}[\mathbf{r}] + \zeta \mathbf{r}\mathbf{r}^T \\ &= \mathbf{I} - \frac{1}{2}[\mathbf{r}] + \zeta[\mathbf{r}]^2 \end{aligned} \tag{25}$$

Remark. Equation (22) can also be derived directly from equation (21) by using the following formula:

$$(x\mathbf{I} + y[\mathbf{r}] + z[\mathbf{r}]^2)(d\mathbf{I} + e[\mathbf{r}] + f[\mathbf{r}]^2) = \mathbf{I} \tag{26}$$

where

$$d = \frac{1}{x} \tag{27}$$

$$e = \frac{-y}{(x - \|r\|^2 z)^2 + \|r\|^2 y^2} \tag{28}$$

$$f = \frac{y^2 - xz + \|r\|^2 z^2}{a\left((x - \|r\|^2 z)^2 + \|r\|^2 y^2\right)} \tag{29}$$

Likewise, equations (23) and (25) can be derived from each other by using equation (26).

Numerically robust computation

Note that although α, β, γ, ζ, and δ are all well-defined at $\theta = 0$, direct use of the previous formulas for $\mathbf{w}_b$ and $\mathbf{w}_s$ involve a division by zero. Instead, for θ close to zero one can evaluate the variables up to machine precision accuracy via the following Taylor series expansion:

$$\alpha = 1 - \frac{\theta^2}{6} + O(\theta^4) \tag{30}$$

$$\beta = \frac{1}{2} - \frac{\theta^2}{24} + O(\theta^4) \tag{31}$$

$$\gamma = \frac{1}{6} - \frac{\theta^2}{120} + O(\theta^4) \tag{32}$$

$$\delta = 1 - \frac{\theta^2}{12} + O(\theta^4) \tag{33}$$

$$\zeta = \frac{1}{12} + \frac{\theta^2}{720} + O(\theta^4) \tag{34}$$

Since the machine epsilon of the single precision floating format is 5.96×10^{-8}, the above Taylor series expansion formulas are accurate in machine precision if they are used when $|\theta| < 0.015$. For the double precision format, the machine epsilon is 1.11×10^{-16}; hence the Taylor expansion formulas are to be used for $|\theta| < 1 \times 10^{-4}$.

Second-order differential relation formulas

We will now present the second-order differential relations between the rotation matrix and the exponential coordinates, which are useful for dynamic analysis of spherical joints. The time derivative of $\mathbf{w}_b$ given $\ddot{\mathbf{r}}$ can be achieved straightforwardly by differentiating equation (6):

$$\dot{\mathbf{w}}_b = \alpha\dddot{\mathbf{r}} + (\gamma\langle\mathbf{r}, \dot{\mathbf{r}}\rangle + \dot{\alpha})\ddot{\mathbf{r}} + (\dot{\beta}\dot{\mathbf{r}} + \beta\ddot{\mathbf{r}}) \times \mathbf{r} + (\dot{\gamma}\langle\mathbf{r}, \dot{\mathbf{r}}\rangle + \gamma(\|\dot{\mathbf{r}}\|^2 + \langle\mathbf{r}, \ddot{\mathbf{r}}\rangle))\mathbf{r} \tag{35}$$

where

$$\dot{\alpha} = (\gamma - \beta)\langle\mathbf{r}, \dot{\mathbf{r}}\rangle \tag{36}$$

$$\dot{\beta} = \frac{\alpha - 2\beta}{\theta^2}\langle\mathbf{r}, \dot{\mathbf{r}}\rangle \tag{37}$$

$$\dot{\gamma} = \frac{\beta - 3\gamma}{\theta^2}\langle\mathbf{r}, \dot{\mathbf{r}}\rangle \tag{38}$$

The inverse relation for the above formula is achieved by differentiating equation (15):

$$\ddot{\mathbf{r}} = \dot{\delta}\mathbf{w}_b + \delta\dot{\mathbf{w}}_b + \frac{1}{2}(\dot{\mathbf{r}} \times \mathbf{w}_b + \mathbf{r} \times \dot{\mathbf{w}}_b) + (\dot{\zeta}\langle\mathbf{r}, \mathbf{w}_b\rangle + \zeta(\langle\dot{\mathbf{r}}, \mathbf{w}_b\rangle + \langle\mathbf{r}, \dot{\mathbf{w}}_b\rangle))\mathbf{r} + \zeta\langle\mathbf{r}, \mathbf{w}_b\rangle\dot{\mathbf{r}} \tag{39}$$

where

$$\dot{\delta} = \frac{1}{\theta^2}\frac{\alpha - 1}{2\beta}\langle\mathbf{r}, \mathbf{w}_b\rangle$$

$$\dot{\zeta} = \frac{1}{\theta^4}\left(\frac{\alpha + 1}{2\beta} - 2\right)\langle\mathbf{r}, \mathbf{w}_b\rangle$$

Using the Jacobian matrix $\mathbf{J}_b$ in equation (20), we can rewrite equation (35) in the form of $\dot{\mathbf{w}}_b = \mathbf{J}_b\ddot{\mathbf{r}} + \dot{\mathbf{J}}_b\dot{\mathbf{r}}$. Then the vector $\dot{\mathbf{J}}\dot{\mathbf{r}}$ is expressed as follows:

$$\dot{\mathbf{J}}_b\dot{\mathbf{r}} = (\dot{\alpha} + \gamma\langle\mathbf{r}, \dot{\mathbf{r}}\rangle)\dot{\mathbf{r}} + \dot{\beta}\dot{\mathbf{r}} \times \mathbf{r} + (\dot{\gamma}\langle\mathbf{r}, \dot{\mathbf{r}}\rangle + \gamma\|\dot{\mathbf{r}}\|^2)\mathbf{r} \tag{40}$$

In the form of $\ddot{\mathbf{r}} = \mathbf{G}_b\dot{\mathbf{w}}_b + \dot{\mathbf{G}}_b\mathbf{w}_b$, the vector $\dot{\mathbf{G}}_b\mathbf{w}_b$ can be derived from equation (39) as

$$\dot{\mathbf{G}}_b\mathbf{w}_b = \dot{\delta}\mathbf{w}_b + \frac{1}{2}\dot{\mathbf{r}} \times \mathbf{w}_b + (\dot{\zeta}\langle\mathbf{r}, \mathbf{w}_b\rangle + \zeta\langle\dot{\mathbf{r}}, \mathbf{w}_b\rangle)\mathbf{r} + \zeta\langle\mathbf{r}, \mathbf{w}_b\rangle\dot{\mathbf{r}} \tag{41}$$

The second-order relations for the spatial velocity are derived in the same manner:

$$\ddot{\mathbf{r}} = \dot{\delta}\mathbf{w}_s + \delta\dot{\mathbf{w}}_s - \frac{1}{2}(\dot{\mathbf{r}} \times \mathbf{w}_s + \mathbf{r} \times \dot{\mathbf{w}}_s) + (\dot{\zeta}\langle\mathbf{r}, \mathbf{w}_s\rangle + \zeta(\langle\dot{\mathbf{r}}, \mathbf{w}_s\rangle + \langle\mathbf{r}, \dot{\mathbf{w}}_s\rangle))\mathbf{r} + \zeta\langle\mathbf{r}, \mathbf{w}_s\rangle\dot{\mathbf{r}} \tag{42}$$

$$\dot{\mathbf{J}}_s\dot{\mathbf{r}} = (\dot{\alpha} + \gamma\langle\mathbf{r}, \dot{\mathbf{r}}\rangle)\dot{\mathbf{r}} - \dot{\beta}\dot{\mathbf{r}} \times \mathbf{r} + (\dot{\gamma}\langle\mathbf{r}, \dot{\mathbf{r}}\rangle + \gamma\|\dot{\mathbf{r}}\|^2)\mathbf{r} \tag{43}$$

$$\dot{\mathbf{G}}_s\mathbf{w}_s = \dot{\delta}\mathbf{w}_s - \frac{1}{2}\dot{\mathbf{r}} \times \mathbf{w}_s + (\dot{\zeta}\langle \mathbf{r}, \mathbf{w}_s\rangle + \zeta\langle \dot{\mathbf{r}}, \mathbf{w}_s\rangle)\mathbf{r} + \zeta\langle \mathbf{r}, \mathbf{w}_s\rangle\dot{\mathbf{r}} \quad (44)$$

Note that the following relations should be used to compute $\dot{\alpha}$, $\dot{\beta}$, $\dot{\gamma}$, $\dot{\delta}$, and $\dot{\zeta}$ around $\theta = 0$:

$$\dot{\alpha} \simeq \left(-\frac{1}{3} + \frac{1}{30}\theta^2\right)\langle \mathbf{r}, \dot{\mathbf{r}}\rangle \quad (45)$$

$$\dot{\beta} \simeq \left(-\frac{1}{12} + \frac{1}{180}\theta^2\right)\langle \mathbf{r}, \dot{\mathbf{r}}\rangle \quad (46)$$

$$\dot{\gamma} \simeq \left(-\frac{1}{60} + \frac{1}{1260}\theta^2\right)\langle \mathbf{r}, \dot{\mathbf{r}}\rangle \quad (47)$$

$$\dot{\delta} \simeq \left(-\frac{1}{6} - \frac{1}{180}\theta^2\right)\langle \mathbf{r}, \dot{\mathbf{r}}\rangle \quad (48)$$

$$\dot{\zeta} \simeq \left(\frac{1}{360} + \frac{1}{7560}\theta^2\right)\langle \mathbf{r}, \dot{\mathbf{r}}\rangle \quad (49)$$

Spherical joint modeling and simulation

The differential relations of a rotation and the exponential coordinates obtained in the previous sections have many application areas where the kinematics and dynamics of a rotation are involved. An important application is dynamic simulation of articulated rigid body systems that include spherical joints.

In this section, we deal with two important issues related with modeling kinematics and dynamics of spherical joints. We first show how the differential relations are effectively used in the joint limit analysis of spherical joints. Then we present a reparametrization scheme to avoid singularities.

Joint limit analysis

Spherical joints usually have limited range of motion due to the collision between the adjacent rigid bodies, and it is necessary to model the joint limits for more accurate kinematic and dynamic analysis. In this section, we derive a compact method to analyze the spherical joint's range limit using the exponential coordinate parametrization.

Let us assume that the joint limit of a spherical joint creates a reach cone represented with a fixed unit axis $\mathbf{p}$ and an angle ϕ $(0 \leqslant \phi \leqslant \pi)$ as illustrated in Figure 1. Defining $\mathbf{p}' = \mathbf{R}\mathbf{p}$ as $\mathbf{p}$ rotated by $\mathbf{R} = \exp([\mathbf{r}])$, the joint limit constraint can be described as an inequality:

$$g(\mathbf{r}) = \langle \mathbf{p}, \mathbf{p}'\rangle - \cos\phi \quad (50)$$

$$= \langle \mathbf{p}, \exp([\mathbf{r}])\mathbf{p}\rangle - \cos\phi \quad (51)$$

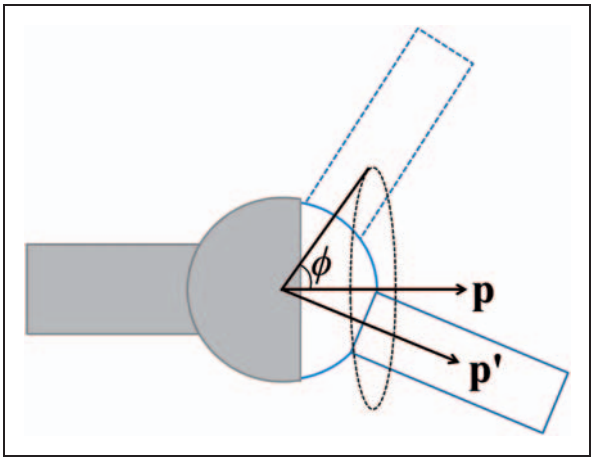

Figure 1. When a joint limit of a spherical joint can be represented with a unit axis $\mathbf{p}$ and angle ϕ, the joint limit constraint can be described in a compact form. $\mathbf{p}'$ is the vector when $\mathbf{p}$ is rotated by $\exp([\mathbf{r}])$.

$$= \cos\theta + \beta\langle \mathbf{r}, \mathbf{p}\rangle^2 - \cos\phi \geqslant 0 \quad (52)$$

Equation (52) is obtained by substituting equation (2) for $\exp([\mathbf{r}])$.

For dynamic simulation, we need to determine the direction of a repulsive impulse when the joint reaches the limit. The impulse direction accounts for the changes in velocity of the adjacent links and is aligned with the gradient direction of $g(\mathbf{r})$. The differential of g can be expressed as

$$\delta g = \langle \mathbf{p}, \delta\mathbf{R}\mathbf{p}\rangle \quad (53)$$

$$= \langle \mathbf{p}, \mathbf{R}[\mathbf{J}_b\delta\mathbf{r}]\mathbf{p}\rangle \quad (54)$$

$$= \langle \mathbf{R}^T\mathbf{p}, [\mathbf{J}_b\delta\mathbf{r}]\mathbf{p}\rangle \quad (55)$$

$$= \langle \mathbf{R}^T\mathbf{p}, -[\mathbf{p}]\mathbf{J}_b\delta\mathbf{r}\rangle \quad (56)$$

$$= \langle \mathbf{J}_b^T[\mathbf{p}]\mathbf{R}^T\mathbf{p}, \delta\mathbf{r}\rangle \quad (57)$$

Hence we obtain the gradient using equations (2) and (20):

$$\nabla g = \mathbf{J}_b^T[\mathbf{p}]\mathbf{R}^T\mathbf{p} \quad (58)$$

$$= (\alpha\mathbf{I} + \beta[\mathbf{r}] + \gamma\mathbf{r}\mathbf{r}^T)(\alpha\mathbf{p} \times (\mathbf{p} \times \mathbf{r}) + \beta\langle \mathbf{p}, \mathbf{r}\rangle(\mathbf{p} \times \mathbf{r})) \quad (59)$$

$$= 2\beta\langle \mathbf{r}, \mathbf{p}\rangle\mathbf{p} - ((\beta^2 - \alpha\gamma)\langle \mathbf{r}, \mathbf{p}\rangle^2 + \alpha)\mathbf{r} \quad (60)$$

At the joint limit, $\langle \mathbf{r}, \mathbf{p}\rangle^2 = \frac{\cos\phi - \cos\theta}{\beta}$ holds from equation (52). Therefore, the gradient at the joint limit is expressed in a compact form as:

$$\nabla g = 2\beta\langle \mathbf{r}, \mathbf{p}\rangle\mathbf{p} - (2\zeta(\cos\phi - \cos\theta) + \alpha)\mathbf{r} \quad (61)$$

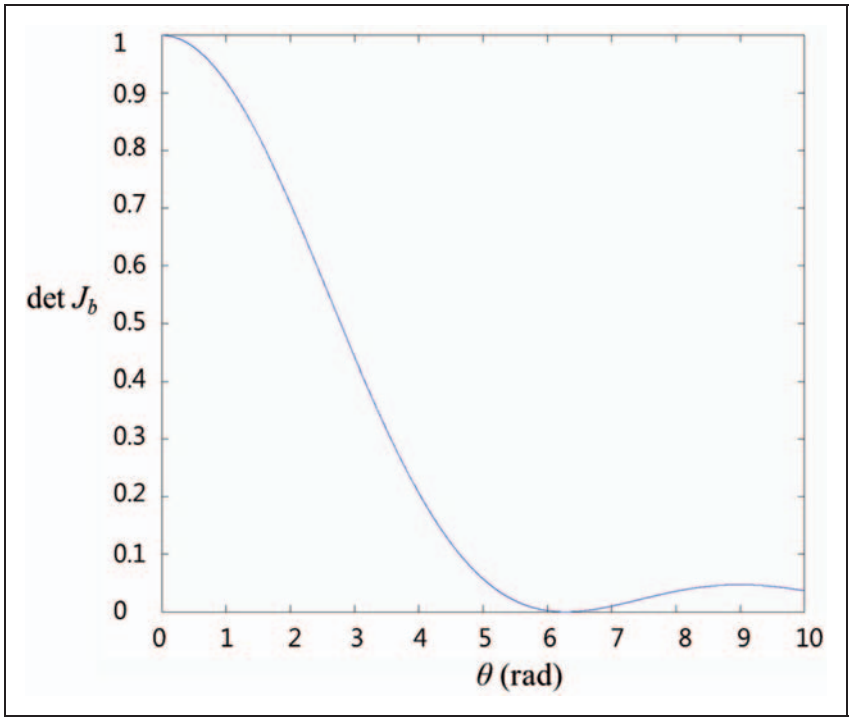

Figure 2. Determinant of $\mathbf{J}_b$ with respect to the rotation angle θ. It is singular $\theta = 2n\pi$ for $n = 1, 2, \ldots$.

Reparametrization

The exponential coordinates representation has singularities like any other three-coordinate parametrization schemes for the rotation group. To examine the singularities, let us calculate the determinant of $\mathbf{J}_b$, which approaches zero as the given parametrization becomes singular. From equation (20), $\mathbf{J}_{bi}$, the i-th column of $\mathbf{J}_b$, is given as

$$\mathbf{J}_{bi} = \alpha \mathbf{e}_i + \beta \mathbf{e}_i \times \mathbf{r} + \gamma \langle \mathbf{r}, \mathbf{e}_i \rangle \mathbf{r} \tag{62}$$

where $\mathbf{e}_i \in \Re^3$ denotes the i-th standard basis vector. Then the determinant of the Jacobian is derived as follows:

$$\det \mathbf{J}_b = \langle \mathbf{J}_{b1} \times \mathbf{J}_{b2}, \mathbf{J}_{b3} \rangle \tag{63}$$

$$= (\alpha^2 + \beta^2 \|\mathbf{r}\|^2)(\alpha + \gamma \|\mathbf{r}\|^2) \tag{64}$$

$$= \frac{2(1 - \cos\theta)}{\theta^2} \tag{65}$$

From equation (65), one can see that the Jacobian is singular at $\theta = 2n\pi$ for $n = 1, 2, \ldots$, but not at $\theta = 0$ (Figure 2). Thus, the exponential coordinates allow for a reasonably wide range of singularity-free configuration of spherical joints. This is a significant advantage of exponential coordinates over Euler angle representations, which have singularities much closer to the default configuration (for example, ZYX Euler angles have a singularity at $(0, \pi/2, 0)$). Therefore, in most practical cases, a spherical joint can never reach the singularity due to the joint limit or other mechanical constraints, and the exponential coordinates can be used without any problem in such cases.

Otherwise, however, one needs to take proper measures to avoid the singularities. One solution is to switch to a different parametrization chart when the original parameter approaches singularity.[7] Recall that rotating about a given axis by an angle of θ results in an identical rotation by an angle of $\theta + 2n\pi \quad (n = 0, \pm 1, \pm 2, \ldots)$, which means $\exp([\mathbf{r}]) = \exp\left([\frac{\theta + 2n\pi}{\theta}\mathbf{r}]\right)$, where $\theta = \|\mathbf{r}\|$. Hence for a given rotation matrix, we can locate the exponential parameter as far as it can be from the singularity by choosing a suitable n.

Let us assume that $\mathbf{r}$ is the current exponential coordinates. If $\pi < \theta < 3\pi$, we can reparametrize the rotation matrix using $\mathbf{r}'$ such that $\|\mathbf{r}'\|$ is bound to $[0, \pi)$ as follows:

$$\mathbf{r}' = \eta \mathbf{r} \tag{66}$$

$$\eta = 1 - \frac{2\pi}{\theta} \tag{67}$$

In general, the formula for selecting n can be defined as follows:

$$n = -\left\lfloor \frac{\lfloor \frac{\theta}{\pi} + 1 \rfloor}{2} \right\rfloor \tag{68}$$

The same formula as equation (66) was also presented in Ref. 7. Here, we extend the reparametrization

scheme to the cases for the dynamic simulation of the spherical joints, in which case it is necessary to reparametrize $\dot{\mathbf{r}}$ and $\ddot{\mathbf{r}}$ as well. By differentiating equation (66) we can derive the first and second derivatives of $\mathbf{r}'$:

$$\dot{\mathbf{r}}' = \eta\dot{\mathbf{r}} + 2\pi\frac{\langle \mathbf{r}, \dot{\mathbf{r}}\rangle}{\theta^3}\mathbf{r} \tag{69}$$

$$\ddot{\mathbf{r}}' = \eta\ddot{\mathbf{r}} + 4\pi\frac{\langle \mathbf{r}, \dot{\mathbf{r}}\rangle}{\theta^3}\dot{\mathbf{r}} + 2\pi\left(\frac{\|\dot{\mathbf{r}}\|^2 + \langle \mathbf{r}, \ddot{\mathbf{r}}\rangle}{\theta^3} - 3\frac{\langle \mathbf{r}, \dot{\mathbf{r}}\rangle^2}{\theta^5}\right)\mathbf{r} \tag{70}$$

We may also need to reparametrize the dual of $\dot{\mathbf{r}}$ when a joint torque is applied to a spherical joint. Let τ and τ' denote the duals of $\dot{\mathbf{r}}$ and $\dot{\mathbf{r}}'$ respectively. From $\langle \tau', \dot{\mathbf{r}}'\rangle = \langle \tau, \dot{\mathbf{r}}\rangle$,

$$\langle \tau', \dot{\mathbf{r}}'\rangle = \langle \tau, \mathbf{J}_b^{-1}\mathbf{w}_b\rangle \tag{71}$$

$$= \langle \tau, \mathbf{J}_b^{-1}\mathbf{J}_b'\dot{\mathbf{r}}'\rangle \tag{72}$$

$$= \langle \mathbf{J}_b'^T\mathbf{J}_b^{-T}\tau, \dot{\mathbf{r}}'\rangle \tag{73}$$

where $\mathbf{J}_b'$ is defined as $\mathbf{w}_b = \mathbf{J}_b'\dot{\mathbf{r}}'$, i.e.,

$$\mathbf{J}_b' = \mathbf{I} - \beta'[\mathbf{r}'] + \gamma'[\mathbf{r}']^2 \tag{74}$$

$$= \mathbf{I} - \frac{\beta}{\eta}[\mathbf{r}] + \frac{1}{\eta}\left(\gamma - \frac{2\pi}{\theta^3}\right)[\mathbf{r}]^2 \tag{75}$$

Therefore, we get

$$\tau' = \mathbf{J}_b'^T\mathbf{J}_b^{-T}\tau \tag{76}$$

$$= \left(\mathbf{I} - \frac{2\pi}{\eta\theta^3}[\mathbf{r}]^2\right)\tau \tag{77}$$

$$= \tau - \frac{2\pi}{\eta\theta^3}\mathbf{r} \times (\mathbf{r} \times \tau) \tag{78}$$

Conclusion

In this paper, numerically robust computational procedures and formulas for spherical joints based on exponential coordinates have been proposed. With exponential coordinates, joint range limits can be easily parametrized in terms of cones, and the direction of the repulsive impulse at joint limits can be obtained in a compact form. Reparametrizations of exponential coordinates and its first and second derivatives as well as the torque near local singularities can be easily formulated. These procedures are performed based on the analytic formulas for the angular velocity and acceleration in terms of exponential coordinates and its first and second derivatives, as well as numerically robust procedures for computing the formulas.

Funding

This work was supported in part by the Korea Institute of Science and Technology under the Tangible Social Media Platform Project, and by the Basic Science Research Program of NRF, Korea (2010-0025725). F. C. Park was supported in part by the Advanced Intelligent Manipulation Center, Biomimetic Robotics Research Center, SNU-IAMD, and SNU-MAE BK21+.

References

1. Mirtich B and Canny J. Impulse-based simulation of rigid bodies. *1995 Symposium on interactive 3D graphics*. 1995, pp.181–188.
2. Kokkevis E and Metaxas D. Efficient dynamic constraints for animating articulated figures. *Multibody Syst Dyn* 1998; 2: 89–114.
3. Bortz JE. A new mathematical formulation for strapdown inertial navigation. *IEEE Trans Aerosp Electron Syst* 1971; 7: 61–66.
4. Nazaroff GJ. The orientation vector differential equation. *J Guid Control* 1979; 2: 351–352.
5. Jiang YF and Lin YP. On the rotation vector differential equation. *IEEE Trans Aerosp Electron Syst* 1991; 27: 181–183.
6. Park FC and Kang IG. Cubic spline algorithms for orientation interpolation. *Int J Numer Methods Eng* 1999; 46: 45–64.
7. Grassia FS. Practical parameterization of rotations using the exponential map. *J Graphics Tools* 1998; 3: 29–48.
8. Bullo F and Murray RM. Proportional derivative (PD) control on the Euclidean group. CDS Technical Report 95-010, California Institute of Technology, USA, 2005, pp.1–47.
9. Selig JM. *Geometric fundamentals of robotics*. New York: Springer Verlag, 2005.
10. Visser M, Stramigioli S and Heemskerk C. Cayley-Hamilton for roboticists. In: *Proceedings of 2006 IEEE/RSJ international conference on intelligent robots and systems*, 2006, pp.4187–4192.
11. Stuelpnagel J. On the parametrization of the three-dimensional rotation group. *SIAM Rev* 1964; 6: 422–430.
12. Gelman H. A note on the time dependence of the effective axis and angle of rotation. *J Res Natl Bur Stand* 1971; 75: 165–171.
13. Savage PG. *Stapdown system algorithms. Advances in strapdown inertial systems*. Lecture Series, 1984, p.133.
14. Hughes PC. *Spacecraft attitude dynamics*. New York: Wiley, 1986.
15. Shuster MD. The Kinematic equation for the rotation vector. *IEEE Trans Aerosp Electron Syst* 1993; 29: 263–267.
16. Ignagni MB. On the orientation vector differential equation in strapdown inertial systems. *IEEE Trans Aerosp Electron Syst* 1994; 30: 1076–1081.
17. Murray RM, Li Z and Sastry SS. *A mathematical introduction to robotic manipulation*. New York: CRC Press, 1994.
18. Park FC, Bobrow JE and Ploen SR. A Lie group formulation of robot dynamics. *Int J Robot Res* 1995; 14: 609–618.

19. Engin AE and Tumer SM. Three-dimensional kinematic modelling of the human shoulder complex—part I: physical model and determination of joint sinus cones. *J Biomech Eng* 1989; 111: 107–112.
20. Tumer SM and Engin AE. Three-dimensional kinematic modelling of the human shoulder complex—part II: mathematical modelling and solution via optimization. *J Biomech Eng* 1989; 111: 113–121.
21. Wilhelms J and Gelder AV. Fast and easy reach-cone joint limits. *J Graphics Tools* 2001; 6: 27–41.
22. Lee S-H and Terzopoulos D. Spline joints for multibody dynamics. *ACM Trans Graphics* 2008; 27: 22:1–22:8.
23. Featherstone R. *Robot dynamics algorithms*. Boston: Kluwer Academic Publishers, 1987.
24. Belta C and Kumar V. Euclidean metrics for motion generation on SE(3). *Proc IMechE, Part C: J Mechanical Engineering Science* 2002; 216: 47–60.